Dynamic magnetization states of a spin valve in the presence of dc and ac currents: Synchronization, modification, and chaos

Z. Li,[1] Y. Charles Li,[2] and S. Zhang[1]
[1]*Department of Physics and Astronomy, University of Missouri-Columbia, Columbia, Missouri 65211, USA*
[2]*Department of Mathematics, University of Missouri-Columbia, Columbia, Missouri 65211, USA*
(Received 19 June 2006; published 16 August 2006)

We present analytical and numerical calculations of dynamic magnetization states of a spin valve in the presence of dc and ac currents. Three distinct dynamic phases, synchronization, modification, and chaos, are identified within the experimental parameter space. A particularly interesting result is the appearance of the synchronization-chaos boundaries. In the region of synchronization, our results agree with experiments. In the modification and chaos regions, we predict experimentally observable power spectra.

DOI: 10.1103/PhysRevB.74.054417 PACS number(s): 75.75.+a, 75.25.+z, 85.75.−d, 05.45.Xt

I. INTRODUCTION

The phenomenon of current-driven steady-state precessional motion of magnetization in nanometer-scale magnetic devices has been understood in terms of spin transfer torques: the nonequilibrium conduction electrons pump in a magnetic energy that exactly compensate the damping loss in a precessional cycle.[1–5] The stabilized magnetization oscillators open new application capabilities in electrical control of nanosized microwave devices. Recently, it is found experimentally that the precessional motion can be either synchronized by an ac current[6] or mutually synchronized by another nearby similar oscillator.[7,8] The successful synchronization of the oscillators greatly enhances the power output and reduces the noise compared to a single oscillator, and thus it is more desirable for an effective application. However, there is a lack of systematical understanding on the nature of the current-driven phase-locking phenomenon. In the nonlinear theory,[9–11] the most important parameters in synchronization are the amplitude of the ac current and the detune frequency (ν) which is defined as the difference between the frequency of the original dc current-driven oscillation and the frequency of the applied ac current. When the parameters are outside the region of synchronization, complicated dynamic phases are expected to appear.

In this paper, we consider a simple spin valve as a model system to study the problem of synchronization and other dynamic phases. Specifically, it is desirable to determine what are the dynamic phases outside the synchronization region for the experimentally available parameter space. The model spin valve consists of a pinned layer whose magnetization is fixed at x axis and a single-domain free layer whose magnetization vector $|\mathbf{m}|=1$ is the subject of our calculation. The dynamics of the free layer magnetization is determined by the standard Landau-Lifshitz-Gilbert (LLG) equation with the addition of a spin transfer torque,[1]

$$\frac{\partial \mathbf{m}}{\partial t} = -\gamma \mathbf{m} \times \mathbf{H}_{\text{eff}} + \alpha \mathbf{m} \times \frac{\partial \mathbf{m}}{\partial t} + (a_{\text{dc}} + a_{\text{ac}} \cos \omega t)\mathbf{m} \times (\mathbf{m} \times \mathbf{e}_x), \quad (1)$$

where a_{dc} and a_{ac} are the amplitudes of the spin torque due to dc and ac currents, respectively, ω is the frequency of the ac current, and the effective field is $\mathbf{H}_{\text{eff}}=H_{\text{ext}}\mathbf{e}_x+H_k m_x \mathbf{e}_x - 4\pi M_s m_z \mathbf{e}_z$. This field consists of the external field and anisotropy, both along the x axis, and a demagnetization field along the z axis. The remainder of the paper is to solve the dynamic phases from Eq. (1). In Sec. II we numerically integrate Eq. (1) and describe several distinct dynamics phases in detail. In Sec. III we provide an analytical proof for the existence of chaos. It is found that the perturbative determination of the corresponding Melnikov integral gives excellent agreement with our numerical results. We discuss our results in Sec. IV.

II. NUMERICAL DETERMINATION OF DYNAMIC PHASES

For our macrospin model where the free layer is a single domain, the numerical integration of Eq. (1) can be straightforwardly carried out. We choose the parameters in Eq. (1) similar to those of a permalloy film: the damping constant $\alpha=0.02$, the anisotropy field is zero, the demagnetization field is $4\pi M_s=8400$ Oe, and gyromagnetic ratio is $\gamma=1.7 \times 10^7$ $(\text{Oe})^{-1}$ s^{-1}. First we identify precessional steady state (also known as the limit cycle) solution without the ac current.[12] The relation between the frequency of the limit cycle and the dc current density is shown as the dotted line in Fig. 1. Note that the decreasing and increasing branches represent two distinct magnetization trajectories known as in-plane and out-of-plane precessional motion.[3] We then consider the magnetization dynamics when an ac current, whose frequency is different from those of the limit cycles, is turned on. We find that the magnetic states appear to have three dynamic phases: synchronization, modification, and chaos. For a fixed amplitude of the ac current, the limit cycle is always synchronized with the external frequency as long as the detune frequency is small. When the detune frequency is not small, two other phases appear: modification and chaos. In Fig. 1, we show the complete dynamic phase diagram for a fixed ac amplitude. We describe each of these phases below.

A. Synchronization

As expected, the synchronization regions, labeled by S of the green stripe, are confined in the vicinity of the original

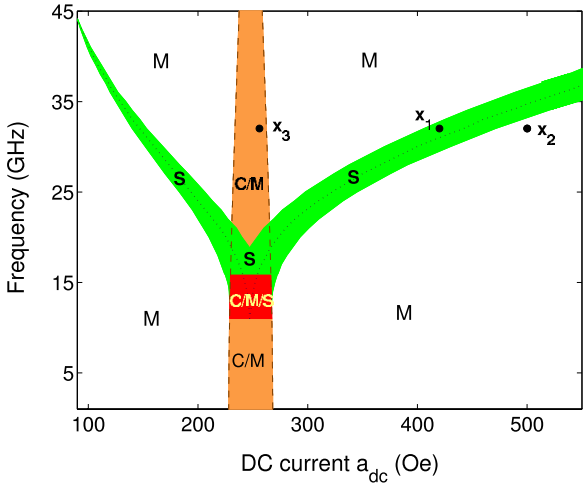

FIG. 1. (Color online) Magnetization dynamic phase diagram driven by dc and ac currents. The external field is fixed at 200 Oe and the amplitude of the ac current a_{ac}=20 Oe. Three phases are synchronization (S), modification (M), and chaos (C). The dotted line is the frequency of the limit cycle in the absence of the ac current. The analytical results from the Melnikov criterion of chaos are shown in the two nearly vertical dashed lines.

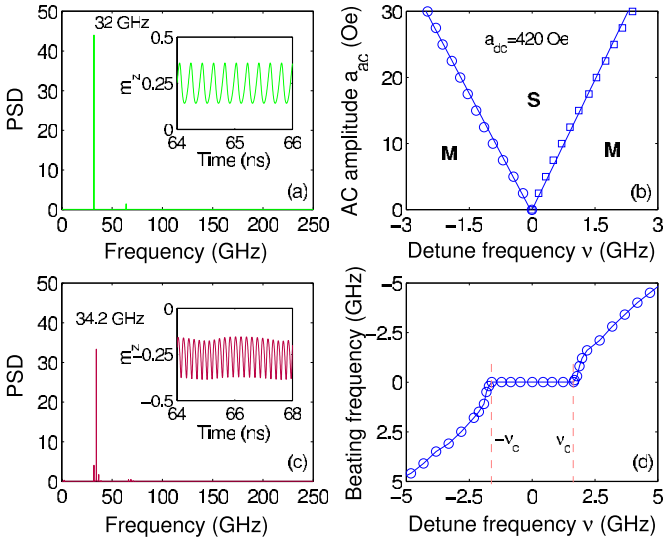

FIG. 2. (Color online) Synchronization and modification of magnetization dynamics. (a) The power spectrum and time trace (inset) for the point "x_1" (a_{dc}=420 Oe, ω=32 GHz) of Fig. 1 in the synchronized region. (b) Synchronization and modification boundaries in the plane of the detune frequency ν and the amplitude of the ac current a_{ac} for a fixed dc current. (c) The power spectrum and the beat phenomenon (inset) for the point "x_2" (a_{dc}=500 Oe, ω=32 GHz, see Fig. 1) in the modification region. (d) The beat frequency as a function of the detune frequency for fixed amplitudes of the dc and ac currents.

frequency of the limit cycle (shown as the dotted line in Fig. 1). When synchronization occurs, the spectrum peak is exactly at the external frequency and consequently the peak is higher but narrower compared to the original spectrum of the limit cycle without the ac current. We take the point "x_1" (a_{dc}=420 Oe, ω=32 GHz) in Fig. 1 to illustrate the time trace and power spectrum for the typical synchronization shown in Fig. 2(a). When we increase the amplitude of the ac current, the width of the synchronization stripe in Fig. 1 increases, i.e., the synchronization region expands. The area of synchronization on the plane of parameters of the detune frequency and the ac amplitude for a fixed dc current is shown in Fig. 2(b). The straight lines of the synchronization boundaries indicate that one can treat the external ac current as a perturbation and analytically determine the phase boundaries as we will show in the next section. Therefore, the experimental observation of synchronization[6–8] can be explained by the general synchronization theory valid for the whole class of nonlinear oscillating systems.[9] We note that an explicit calculation for the synchronization region was also carried out previously in a different content.[13,14]

B. Modification

The loss of exact synchronization occurs where the detune frequency ν increases to a critical value ν_c. In this region, the time trace of the magnetization shows fast and slow oscillations; the latter are known as the "beat phenomenon." In Fig. 2(c), we depict the time trace and power spectrum for the typical modification. The frequency where the power spectrum is peaked is different from the external frequency and their difference is defined as the beat frequency. It is noted that the beat frequency in this modification region is *not* the beat frequency of a linear system which is simply the difference between the nature frequency and the driving frequency. For the point "x_2" (a_{dc}=500 Oe, ω=32 GHz) in Fig. 1, the beat frequency is about 2.2 GHz. We show in Fig. 2(d) the beat frequency as a function of the detune frequency. When the detune frequency is smaller than ν_c, the beat frequency is exactly zero, i.e., exact phase locking. When $|\nu| > \nu_c$, the nonzero beat frequency begins to appear. One may analytically investigate the relation of the beat frequency as a function of the detune frequency for a weakly perturbed nonlinear oscillator.[9] In general, the beat frequency is proportional to $\sqrt{|\nu|-\nu_c}$ when the detune frequency ν is just outside the synchronization region. Both the prediction of the synchronization area and of the linear dependence of ν and a_{ac} are in excellent agreement with experiments.[6]

C. Chaos

The most interesting dynamic phase is the ac current-driven chaos. One immediately notices from the phase diagram of Fig. 1 that the chaos occurs in a narrow stripe where the frequency of the dc current is near the vicinity of the frequency minimum of the limit cycle. Solving inequality Eq. (7) or Eq. (8) to be described later, one can obtain the chaos boundary shown in the two nearly vertical dashed lines shown in Fig. 1. The agreement of our analytical and numerical predictions of chaos in the stripe is almost perfect. The time trace of magnetization shown in Figs. 3(a) and 3(b) clearly displays the chaotic bouncing between the two original limit cycles: one above and one below the layer plane for the same parameters. Without the ac current, these two degenerate limit cycles are independent. For a given initial

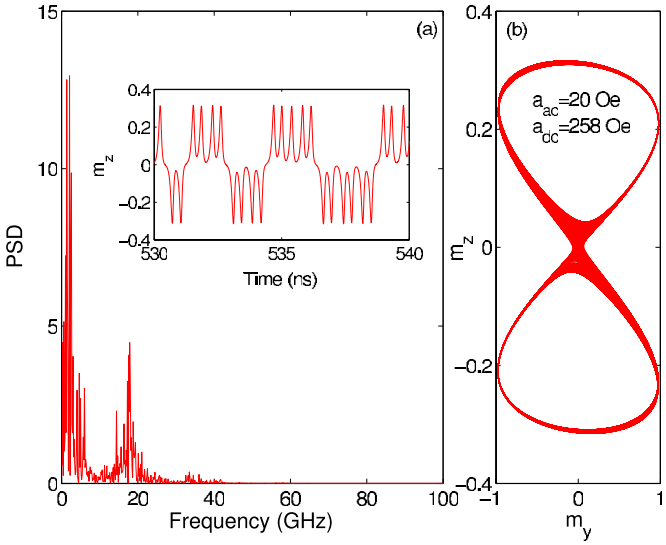

FIG. 3. (Color online) Chaotic magnetization dynamics. (a) The power spectrum and the time trace (inset) of the point "x_3" (a_{dc} =258 Oe, ω=32 GHz, see Fig. 1) at the chaotic region. (b) The two-dimensional plot of the chaotic magnetization orbital showing typical chaotic motion.

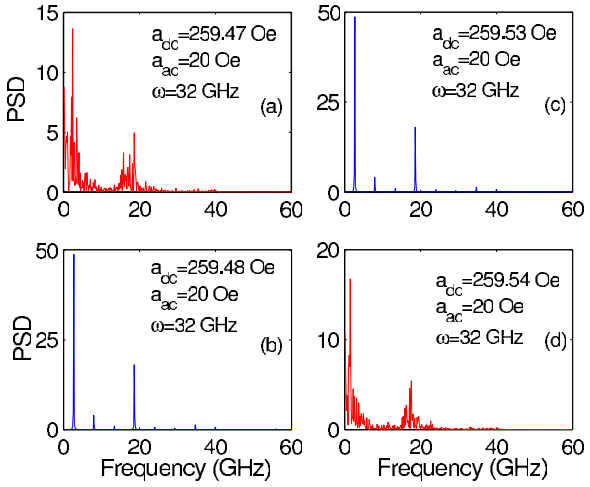

FIG. 4. (Color online) The window of magnetization dynamics. With small increments of a_{dc}, the power spectra change from chaotic [(a) a_{dc}=259.47 Oe] to modification [(b) a_{dc}=259.48 Oe], then from modification [(c) a_{dc}=259.53 Oe] back to chaos [(d) a_{dc} =259.54 Oe].

magnetization vector, only one of these two limit cycles is able to attract the magnetization trajectory. In the presence of the ac current, the magnetization jumps back and forth from one to the other. Another key difference between the chaos phase and the other two phases is that the power spectrum of the chaos phase shows no well-defined peaks shown in Fig. 3(a). We have also performed a numerical evaluation of the Liapunov characteristic exponents to support our notion that the dynamics is a true chaos.[15]

We point out that the chaos driven by the periodic ac current is fundamentally different from the magnetization chaos due to spatially nonuniform magnetization dynamics reported in the micromagnetic simulation by Lee *et al.*[16] In the latter case, the dc current alone generates spin waves with different wavelengths due to nonuniform magnetostatic interaction. The nonuniform magnetization appears spatially chaotic, or enhanced noise. It is nearly impossible to analyze the characteristics of these chaotic dynamics since the sample size and geometry play the key roles. When the sample size is sufficiently small, the nonuniform magnetization induced chaos (or noise) will be completely suppressed.

D. Windows and weaker chaos

Although we have proved rigorously below the existence of chaos in the stripe by treating the Gilbert damping and the spin torque as perturbations, the stability of the chaos is a challenging issue that cannot be dealt with mathematically. From numerical simulations, often chaos can lose and regain its stability over small parameter intervals. The small parameter interval where chaos loses its stability and another simpler attractor gains stability, is called a window. With small increments of the dc current, the power spectra change from chaotic to modification and then back to chaotic, as shown in Fig. 4. Indeed, a small variation of the parameters (e.g., dc current or damping parameter) may produce different phases in the regions of C/M or $C/M/S$, our numerics found several windows in the chaos stripe as shown in Fig. 5(a). Inside the window, a modification or synchronization state is the attractor. Near the boundaries of the window, the modification or synchronization often undergoes a Hopf bifurcation[17] before it enters the chaos region. Sometimes such an initial chaos region supports chaos around only one of the two loops. The chaos in the stripe is generated from a separatrix (also loosely defined as fixed points) which exists even when the Gilbert damping and the spin torque are dropped. On the

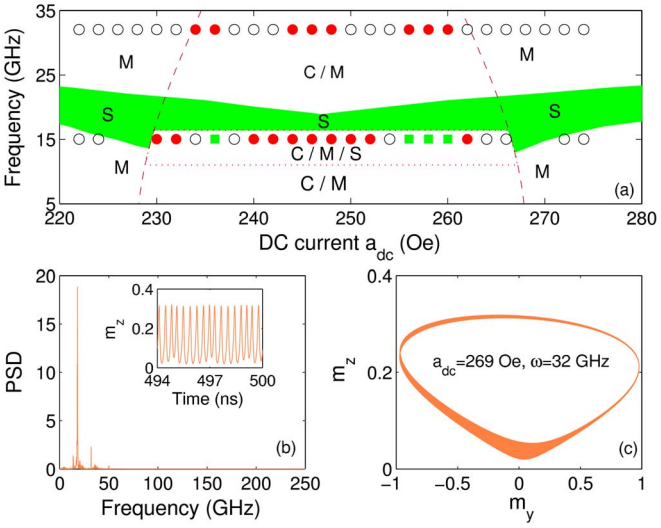

FIG. 5. (Color online) (a) Magnetic phase variation across C/M and $C/M/S$ regions. Solid red circles, solid green squares, and hollow white circles represent dynamics of chaos, synchronization and modification, respectively. (b) The power spectrum and the time trace (inset) of the point (a_{dc}=269 Oe, ω=32 GHz) at the weaker chaotic window. (c) The two-dimensional plot of the magnetization orbital showing the weaker chaotic motion.

other hand, the ac current can generate parametric instabilities which can lead to weaker chaos. Our numerics has indeed detected such weaker chaos outside the chaos stripe [not shown in Fig. 5(a)]. A complete understanding of windows and weaker chaos may require further investigation and we do not have an analytical determination of when and how these phases appear in this region. In Figs. 5(b) and 5(c), we depict the time trace, the power spectrum, and the two-dimensional magnetization orbital for the typical weaker chaos.

III. MATHEMATICAL PROOF OF THE EXISTENCE OF CHAOS

While both synchronization and modification are expected for any nonlinear oscillator with a periodic driven force, the presence of chaos is not a universal property of nonlinear oscillators. In the following, we provide a rigorous mathematical proof of the existence of chaos for our simple spin valve system. For the notational simplicity, we rewrite Eq. (1) in terms of dimensionless parameters normalized by $4\pi M_s$ for the external field, anisotropy field, and currents,

$$h_e = \frac{H_{\text{ext}}}{4\pi M_s}, \quad h_k = \frac{H_k}{4\pi M_s}, \quad \beta_1 = \frac{a_{\text{dc}}}{4\pi M_s}, \quad \beta_2 = \frac{a_{\text{ac}}}{4\pi M_s}. \tag{2}$$

Setting $\alpha=0$ and $\beta_{1,2}=0$, the magnetization orbit given by the first term in Eq. (1) conserves the magnetic energy (normalized by $4\pi M_s^2$), $E_0=-h_e m_x - h_k m_x^2/2 + m_z^2/2$. It is noted that there may exist more than one orbit for a given energy E_0.

Calculating separatrices connected to a saddle point ($m_x=-1$, $m_y=0$, $m_z=0$), one can obtain a pair of homoclinic orbits in the parameter range of $h_k < h_e < h_k+1$,

$$m_x = M_0 - 1 = \frac{4C_1 e^{-\tau}}{(e^{-\tau} - C_2)^2 - 4C_1 C_3},$$

$$m_y = \pm\sqrt{M_0[2(h_k+1-h_e) - (h_k+1)M_0]},$$

$$m_z = \pm\sqrt{M_0[2(h_e-h_k) + h_k M_0]}, \tag{3}$$

where

$$\tau = \sqrt{C_1}(t_1 + t_0), \quad t_1 = 4\pi M_s \gamma t,$$

$$C_1 = 4(h_e - h_k)(h_k + 1 - h_e),$$

$$C_2 = 2[h_k(h_k+1-h_e) - (h_e-h_k)(h_k+1)],$$

$$C_3 = -h_k(h_k+1)$$

in which t_0 is a real parameter. It is found that the pair of homoclinic orbits are asymptotic to the saddle point when $t \to \pm\infty$.

When we include the other terms in Eq. (1), the energy of the orbit is no longer a constant. To prove that the pair of homoclinic orbits persist when $\alpha \neq 0$ and $\beta_{1,2} \neq 0$, one needs to build a Melnikov integral (Melnikov theorem[18]),

$$G = E_0 + \frac{h_k - h_e}{2}(m_x^2 + m_y^2 + m_z^2). \tag{4}$$

The Melnikov integral is given by

$$U = -\alpha U_1 + \beta_1 U_2 + \beta_2 \cos\left(\frac{\omega t_0}{4\pi M_s \gamma}\right) U_3 + \beta_2 \sin\left(\frac{\omega t_0}{4\pi M_s \gamma}\right) U_4, \tag{5}$$

where

$$U_1 = \int_{-\infty}^{+\infty} \nabla G \cdot [\mathbf{m} \times (\mathbf{m} \times \mathbf{H}_{\text{eff}})] d\tau,$$

$$U_2 = \int_{-\infty}^{+\infty} \nabla G \cdot [\mathbf{m} \times (\mathbf{m} \times \mathbf{e}_x)] d\tau,$$

$$U_3 = -\int_{-\infty}^{+\infty} \cos\left(\frac{\omega\tau}{4\pi M_s \gamma\sqrt{C_1}}\right) \nabla G \cdot [\mathbf{m} \times (\mathbf{m} \times \mathbf{e}_x)] d\tau,$$

$$U_4 = -\int_{-\infty}^{+\infty} \sin\left(\frac{\omega\tau}{4\pi M_s \gamma\sqrt{C_1}}\right) \nabla G \cdot [\mathbf{m} \times (\mathbf{m} \times \mathbf{e}_x)] d\tau$$

are evaluated along the homoclinic orbits to Eq. (3).

In general, the simple zero of the Melnikov integral implies the existence of a homoclinic orbit. Around the homoclinic orbit, chaos is often generated.

Setting $U=0$, one obtains that

$$\cos\left(\frac{\omega t_0}{4\pi M_s \gamma} - \psi\right) = \frac{\alpha U_1 - \beta_1 U_2}{\beta_2\sqrt{U_3^2 + U_4^2}}, \tag{6}$$

where

$$\cos\psi = \frac{U_3}{\sqrt{U_3^2 + U_4^2}}, \quad \sin\psi = \frac{U_4}{\sqrt{U_3^2 + U_4^2}}$$

thus as long as

$$|\alpha U_1 - \beta_1 U_2| \leqslant |\beta_2|\sqrt{U_3^2 + U_4^2}, \tag{7}$$

U has zeros. Direct calculation shows that the zeros of U lie in the vertical band region in Fig. 1. The standard arguments of existence of a pair of transversal homoclinic orbits lead to the following theorems.

A. Homoclinic orbit theorem

There exists a δ $(0 < \delta \ll 1)$, such that whenever α and $\beta_{1,2}$ are small, and

$$|\beta_2| \geqslant \frac{|\alpha U_1 - \beta_1 U_2|}{\sqrt{U_3^2 + U_4^2}} + \delta \tag{8}$$

there is a pair of transversal homoclinic orbits to Eq. (1).

Let P be the Poincaré period 2π map, $P: S^2 \mapsto S^2$, where S^2 is the 2-sphere. Under the map P, the pair of transversal

homoclinic orbits turns into a pair of discrete transversal homoclinic orbits. Using shadowing lemma technique, one can prove the following chaos theorem. The proof is standard.[18,19]

B. Chaos theorem

In the neighborhood of the pair of transversal homoclinic orbits, there is a Cantor subset Λ of S^2. Λ is invariant under the Poincaré period 2π map P. P restricted to Λ is topologically conjugated to the Bernoulli shift on two symbols.[18,19]

IV. DISCUSSIONS AND CONCLUSIONS

We have shown that there are three distinct dynamic phases driven by an external ac current. The external periodic force can be in other forms. For example, one can apply an ac magnetic field instead of the ac current. A similar phase diagram would be obtained. In fact, we suggest that dynamic phases driving by the ac magnetic field are easily experimentally accessible since the ferromagnetic resonance which uses a rf field and a large static field to probe the magnetization relaxation has been routinely done for many decades. Thus we propose that a study of dynamic phases by a rf field would test the spin torque theory quantitatively.

The most interesting dynamic phase is chaos. We have calculated the chaos at zero temperature. An immediate concern is the chaos at the finite temperature. As the thermal fluctuation can make the transition from one orbital to another[20] and thus lead to the spectrum similar to Fig. 3, one wants to distinct the chaos driven by an external periodic force with that due to thermal fluctuation. Experimentally, one can readily separate these two chaos by following hypothetical experiments: (1) By varying any amplitude (frequency) of ac, dc currents or magnetic fields, the power spectrum would change from nonchaotic to chaotic and back to nonchaotic; this feature does not exist for thermal driven chaos. (2) By varying temperature, the external periodic force driven chaos is not affected while the thermal driven chaos is completely changed. (3) The thermal driven chaos can occur in a wide range of the orbits while the periodic force driven chaos is confined to rather narrow space of precessional orbits as shown in our phase diagram, Fig. 1.

Until now, we have only considered the dynamic phases without including noise or chaos presented in the limit cycle. The interesting challenge in modern synchronization is the phase locking for chaotic systems. We may extend our study in two ways. First, we introduce a finite temperature so that the dynamics of the limit cycle without the ac current is chaotic. It will be interesting to study how the phase locking occurs when an ac current turns on.[21] The second interesting case is to study the phase locking between two chaotic oscillators (limit cycles). In this case, the rich dynamic structure would be expected. For example, the two chaotic limit cycles have a perfect phase locking but have completely uncorrelated and chaotic amplitudes.[22,23] We defer these interesting cases for a further study.

In conclusion, by using both analytical and numerical approaches, we show that the magnetic states in the presence of the dc and ac currents have three distinct phases: (a) synchronization when the exact phase locking of the oscillator and the external ac current occurs, (b) modification when the oscillator and the external ac frequency show the "beat" phenomenon, and (c) chaos when the trajectory of the magnetization undergoes chaotic motion. Our quantitative theory provides detailed tests for experimental verification of the basic spin transfer torque formulation and the magnetic dynamic phases can be broadly used for designing emerging nanomagnetic devices.

ACKNOWLEDGMENT

This work was supported by NSF Grant No. (DMR-0314456).

[1] J. C. Slonczewski, J. Magn. Magn. Mater. **159**, L1 (1996).
[2] M. Tsoi, A. G. M. Jansen, J. Bass, W.-C. Chiang, V. Tsoi, and P. Wyder, Nature (London) **406**, 46 (2000).
[3] S. I. Kiselev, J. C. Sankey, I. N. Krivorotov, N. C. Emley, R. J. Schoelkopf, R. A. Buhrman, and D. C. Ralph, Nature (London) **425**, 380 (2003).
[4] W. H. Rippard, M. R. Pufall, S. Kaka, S. E. Russek, and T. J. Silva, Phys. Rev. Lett. **92**, 027201 (2004).
[5] I. N. Krivorotov, N. C. Emley, J. C. Sankey, S. I. Kiselev, D. C. Ralph, and R. A. Buhrman, Science **307**, 228 (2005).
[6] W. H. Rippard, M. R. Pufall, S. Kaka, T. J. Silva, S. E. Russek, and J. A. Katine, Phys. Rev. Lett. **95**, 067203 (2005).
[7] S. Kaka, M. R. Pufall, W. H. Rippard, T. J. Silva, S. E. Russek, and J. A. Katine, Nature (London) **437**, 389 (2005).
[8] F. B. Mancoff, N. D. Rizzo, B. N. Engel, and S. Tehrani, Nature (London) **437**, 393 (2005).
[9] A. Pikovsky, M. Rosenblum, and J. Kurths, *Syncronization: A Universal Concept in Non-linear Sciences* (Cambridge University Press, Cambridge, 2001).
[10] R. A. York, IEEE Trans. Microwave Theory Tech. **41**, 1799 (1993).
[11] M. I. Rabinovich and D. I. Trubetskov, *Oscillations and Waves in Linear and Nonlinear Systems* (Kluwer, Dordrecht, 1989).
[12] G. Bertotti, C. Serpico, I. D. Mayergoyz, A. Magni, M. d'Aquino, and R. Bonin, Phys. Rev. Lett. **94**, 127206 (2005).
[13] A. N. Slavin and V. S. Tiberkevich, Phys. Rev. B **72**, 092407 (2005).
[14] J. Grollier, V. Cros, and A. Fert, Phys. Rev. B **73**, 060409(R) (2006).
[15] The Liapunov characteristic exponents describe how the distance between two points $x_1(t)$, and $x_2(t)$, with an arbitrary small initial value $|x_1(0)-x_2(0)|<\epsilon$, grows as a function of time. The positive exponent lends a hint that the magnetization dynamics is chaotic since the $|x_1(t)-x_2(t)|$, exponentially grows. For detail, see A. J. Lichtenberg and M. A. Lieberman, *Regular and Stochastic Motion* (Spinger-Verlag, New York, 1983).

[16] K. J. Lee, A. Deac, O. Redon, J. P. Nozières, and B. Dieny, Nat. Mater. **3**, 877 (2004).
[17] J. K. Hale and H. Kocak, *Dynamics and Bifurcations* (Springer-Verlag, New York, 1991).
[18] Y. Li, *Chaos in Partial Differential Equations* (International Press, Bristol, 2004).
[19] K. Palmer, Dyn. Rep. **1**, 265 (1988).
[20] Z. Li and S. Zhang, Phys. Rev. B **68**, 024404 (2003).
[21] G. V. Osipov, B. Hu, C. Zhou, M. V. Ivanchenko, and J. Kurths, Phys. Rev. Lett. **91**, 024101 (2003).
[22] M. G. Rosenblum, A. S. Pikovsky, and J. Kurths, Phys. Rev. Lett. **76**, 1804 (1996).
[23] M. C. Romano, M. Thiel, J. Kurths, I. Z. Kiss, and J. L. Hudson, Europhys. Lett. **71**, 466 (2005).